Interface Structure of Ag/SnO$_2$ Nanocomposite Fabricated by Reactive Synthesis

Jingchao Chen[1), *Jing Feng*[1)†], *B. Xiao*[2), *K.H. Zhang*[1), *Y.P. Du*[1), *Z.J. Hong*[1) *and R. Zhou*[1)]

1) Key Laboratory of Advanced Materials of Precious-Nonferrous Metals, Education Ministry of China, and Key Lab of Advanced Materials of Yunnan Province, Kunming University of Science and Technology, Kunming 650093, China
2) State Key Laboratory of Mechanical Behavior of Materials, School of Materials Science and Engineering, Xi′an Jiaotong University, Xi′an 710049, China

The electric contact material of Ag/SnO$_2$ composite was achieved by reactive synthesis method. The compositions and microstructure of Ag/SnO$_2$ composite were analyzed and characterized by X-ray diffraction (XRD), scanning electron microscopy (SEM), and high-resolution electron microscopy (HRTEM). The structural feature was typical of the particle reinforced composites. The HRTEM images revealed that the observed Ag/SnO$_2$ interface was absence of the precipitated phase and the lattice contrast across the interface was clear and sharp. The average particle size of SnO$_2$ in composite was near 50 nm and it was well dispersed in spherical shape. The thermodynamic mechanism of reactive synthesis method was also discussed. The electronic density distribution analysis of the interface showed the charges of Ag atoms transmitted to O atoms and the conductivity of the material was also affected. No extra compounds expected such as Ag$_x$O$_y$ formed at interface. The distribution of electrons was of inequality near the interface which explained why the mechanical property of the metal/ceramic materials was improved but the machining property declined.

KEY WORDS: Metal-matrix composites; Electric contact material; Interface; *In situ*

1. Introduction

Silver and tin alloy have been frequently used in a variety of industrial applications, such as lead free solders, electric contact materials, gas-sensitive sensor *etc*[1,2]. The metal oxides and other multi-component compounds are usually observed in electric contact materials. Interfaces between ceramic and metallic phases are prominent features in many technologically important materials, and understanding their structure and properties is therefore of considerable interest[3–7]. Considerable attentions have been paid to oxide particles reinforced silver composites due to their important applications in electric equipments as electric contact materials[8,9]. Ag/CdO composite has excellent performance and can be fabricated

easily into many electric devices. However, as Cd is a hazardous element and also due to other environmental concerns, Cd free electric contact materials are now emphasized and studied extensively by many researchers[10]. Ag/SnO$_2$ composite should be one of the most important candidates for such purpose. On the other hand, a few reports indicated that Ag/SnO$_2$ composite was successfully synthesized by equilibrium or non-equilibrium methods, such as powder metallurgy, alloy internal oxidation, reacting spray, chemical plating, reaction synthesis, and reaction ball milling technique[11–14]. Each of these methods shows specific advantages and drawbacks. For example, weakly bonded interfaces of SnO$_2$ and Ag matrix have been observed by powder metallurgy at high temperature. Particularly silver tin oxides (Ag/SnO$_2$) are much more difficult to be fabricated because of poor metallurgical properties[10]. Chen[13] and Feng[14] reported that good mechani-

† Corresponding author. Prof.; Tel.: +86 013888185919;
E-mail address: chenjingchao@kmust.edu.cn (J.C. Chen), vd-mzsfj@sina.com (J. Feng).

cal and electrical performances of Ag/SnO$_2$ composite were achieved by reactive synthesis method. In these silver metal oxides of electronic contact materials, metal/ceramic interfaces exist widely and play an important role in determining the structural, electronic and other properties, *etc.* A fundamental understanding of meta/ceramic interfaces has been elusive, despite their technological importance[15–17]. Considerable experimental progress has been made with the measurement of the atomic structure of several model ceramic/metal interfaces, particularly by high-resolution electron microscopy (HRTEM)[18–21]. Yet many theoretical studies related to this field have been performed, most of which are done by *ab initio* calculations. For example, the Ni/SiC(100) interfaces have been studied by Profeta *et al.*[2,3]. In general, an *ab initio* method is a powerful tool in gaining insight into the electronic and basic structural properties of some interfaces. Furthermore, computer simulation is able to elucidate the electronic structure of ceramic/metal interfaces[7]. In this paper, the new method was applied to prepare silver-tin oxide nanocomposite. The compositions and microstructures of Ag/SnO$_2$ composite were analyzed and characterized. The mechanism of reactive synthesis method and the interface were also discussed.

2. Experimental Methods

The ingredients of the raw materials were listed below: Ag$_2$O (99.0%, 4–5 μm), AgSn alloy powder (Sn: 15.0 wt pct), Ag (99.96%, 45 μm). Reactive synthesis method was adopted. The initial powder-mixtures were carefully prepared. The whole preparation process contained the following steps: powder mixed-powder formed-reactive synthesis (sintering at the temperature 873 K, the equilibrium O$_2$ partial pressure 10^{-1} Pa)-extrusion and drawing wires. Phase identification was carried out by X-ray diffraction (XRD) analysis (220 V, D8-Advance, AXS, Germany). The microstructure was observed by scanning electron microscopy (SEM) (30 kV, XL 30 ESEM, PHLIPS, Holland) and high resolution transmission electron microscopy (HRTEM) (TECNAI G2 F20, FEI, USA).

The whole researches were carried out by using first-principles calculations based on density functional theory (DFT) as implemented in CASTEP code[22]. Ultrasoft pseudo potentials were employed to represent the interactions between ionic core and valence electrons. The exchange correction energy was calculated by the generalized gradient-corrected approximation (GGA) scheme[23–25]. The average forces acting on ions were finally reduced to 1.0×10^{-6} eV/atom. Monkhorst-Pack scheme was used for k point sampling in the first irreducible Brillouin zone (BZ), and 8×8×6 was used for all structures. Valence electrons included in this study for distinct atoms were O 2s^2 2p^4, Ag 4d^{10} 5s^1 and
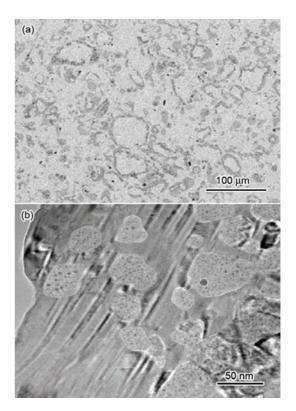

Fig. 1 Scanning electron microscopy images of the as prepared Ag/SnO$_2$ nano-composite, (a) planar element distribution map illustrated with BSE contrast; (b) SEM image of surface morphology

Sn 5s^2 5p^2. The maximum energy cutoff value was 380.0 eV for plane wave expansions. The model′s lattice built on the experiment results, such as Ag: $a=b=c=0.40857$ nm, $\alpha=\beta=\gamma=90°$, SnO$_2$: $a=b=0.47373$ nm, $c=0.31864$ nm, $\alpha=\beta=\gamma=90°$. The structure interface of Ag/SnO$_2$ was observed by HRTEM in reactive synthesis progress. The thickness of the interface structure was about 10 nm and includes 16 layers of atoms, such as 6 layers of Ag and 10 layers of SnO$_2$ (the total number layers of Sn and O atoms). In fact, atom layers outside of 16 layers were fixed.

3. Microstructures of Ag/SnO$_2$ Composite

The microstructures of Ag/SnO$_2$ composite were observed by SEM. Figure 1(a) and (b) respectively illustrate the planar element distribution map and micro-morphology of Ag/SnO$_2$ composite. In Fig. 1(a), the matrix of Ag refers to light regions, and small gray spots are SnO$_2$ particles. Some circlet structures which are surrounded by SnO$_2$ shells were also observed. This feature is very typical of the particle reinforced composites which is fabricated by reactive synthesis method. The average particle size of SnO$_2$ in composite is near 50 nm. Figure 2 depicts the transmission electron microscopy (TEM) images of Ag/SnO$_2$ nanocomposite. It shows the interface structure between SnO$_2$ particle and matrix.
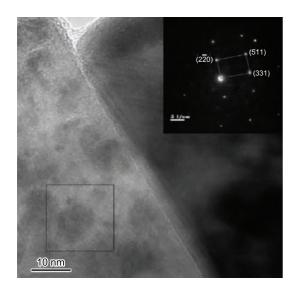
Fig. 2 TEM images of Ag/SnO$_2$ composite: An interface of SnO$_2$ phase and matrix of Ag, the composite at atomic scale to indicate the interface structures between matrix and SnO$_2$ particles

Smooth interface morphology clearly indicates a co-herent or semi-coherent lattice matching relations between reinforced particle and matrix. The inset figure in Fig. 2 shows the electron diffraction pattern of composite. More details of atomic configurations at the interface can be seen in Fig. 3. The observed lattice contrast image implies that no-elements segregation occurs and new phase precipitated at the interface.

4. Discussion

4.1 Thermodynamic mechanism of reactive synthesis of Ag/SnO$_2$ nano-composite

In this part, the mechanism of reactive synthesis of Ag/SnO$_2$ nano-composite will be discussed in detail. During the fabrication of Ag/SnO$_2$ nano-composite, the following reactions could dominate the whole process:

$$Ag_2O = 2Ag + 1/2O_2 \tag{1}$$
$$Sn + 1/2O_2 = SnO \tag{2}$$

$$SnO + 1/2O_2 = SnO_2 \tag{3}$$
$$Sn + O_2 = SnO_2 \tag{4}$$
$$2Ag_2O + Sn = 4Ag + SnO_2 \tag{5}$$

When considering the thermodynamic aspect of chemical reaction, we can evaluate the reactive Gibbs free energy per volume for each of these reactions by Eq. (6)[13]:

$$\Delta GV^\theta = \Delta GV^\theta / V = (H - TSV^\theta) \times \rho/M \tag{6}$$

$$\Delta GV = \Delta GV^\theta + 2.303 RT \lg K \tag{7}$$

All of the thermodynamic data used in this study are cited in literature [26, 27]. We calculated the reactive Gibbs free energy values as a function of temperature from 300 K up to 1200 K. The results are depicted in Fig. 4. It is evident that reaction (2), (3) and (4) could occur at all temperature scale. However, the decomposition of Ag$_2$O is hampered due to positive reactive Gibbs free energy value of reaction (1) below 505 K. Therefore, reaction (5) is the only possible path for the preparation of Ag/SnO$_2$ composite which corresponds to a substitional reaction between two solids, Ag$_2$O and Sn. In the temperature range from 300 K to 505 K, the calculated reactive Gibbs free energy value of Eq. (5) is $\Delta GV^\theta = -22.49$ kJ/cm^{-3}, which implies that it can be conducted spontaneously. When the temperature rise above 505 K, free oxygen atoms were released by decomposition of Ag$_2$O. As a result, all of these proposed reactions could be the possible ways for the formation of Ag/SnO$_2$ composite. On the other hand, as shown in Fig. 5, the smallest reactive Gibbs free energy value corresponds to reaction (4), hence the free oxygen atoms react with Sn directly to produce SnO$_2$ particles. The evaluated reactive Gibbs energy value of reaction (4) is from -22.27 to -15.42 kJ^{-1}·cm^{-3}. Due to the aforementioned reasons, when the reactive temperature was above 505 K, the formation of SnO$_2$ phase in Ag matrix is totally determined by reactions (1)–(4). In other words, in the temperature range of 505 K to 1200 K, these reactions are greatly enhanced by the existence of ex-
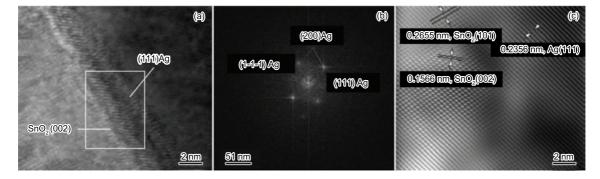

Fig. 3 (a) HRTEM microstructure of Ag/SnO$_2$ composite, (b) electronic diffraction of interface structure in Ag/SnO$_2$ composite, (c) Ag/SnO$_2$ interface lattice fringe image
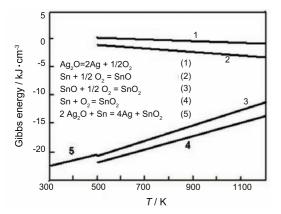
Fig. 4 Reactive Gibbs free energy value plotted as a function of temperature for different reactions, respectively
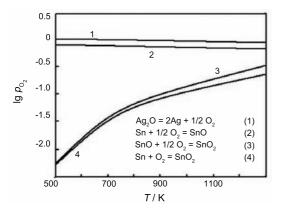

Fig. 5 Relationship between $\lg p_{O_2}$ and temperature of SnO_2 prepared by reactive synthesis

cessive O_2 atmosphere. However, reaction (5) cannot be excluded as we only considered the thermodynamic aspect for the whole process. Kinetical aspects of these reactions also play a key role, which is closely related to dynamical diffusion process of oxygen and tin atoms. Figure 5 shows the effect of the equilibrium O_2 partial pressure on the preparation of Ag/SnO_2 nanocomposite through reactive synthesis method. Equation (7) defines the relationship between the partial pressure of O_2 and the reactive temperature. As illustrated in Fig. 5, (1) and (2) are less affected by partial pressure of O_2, but by contrast it is more to reactions (3) and (4). The equilibrium O_2 partial pressure value increases with increasing the reactive temperature. This indicates that excessive amount of O_2 gas should be involved in order to promote the formation of SnO_2 phase.

4.2 Interface characteristic in Ag/SnO_2 nanocomposite by reactive synthesis

Figure 3 shows the results of HRTEM, which describes the microstructure of the composite synthesized by *in situ* progress. Because the raw materials are Ag_2O and Ag-Sn alloys, the small particles

of SnO_2 are grown *in situ*; the observed interfaces are clear and tightly bonded[13]. The crystal orientations of the Ag/SnO_2 interface are investigated by selected area electron diffraction method. By analyzing the element of interface area, it is found that the boundary is made up of Ag matrix and SnO_2 particles. When compared with the pure crystal, the atoms in the interface were distorted and as a result the interface could be recon-structured during the preparation. On one hand, the internal stresses of the distinct atoms at or near the interface are reduced through structural relaxation. The disparate types of bonding on the opposite sides of the interface pose is particularly true for interfaces of polar character, where the atomic layers on the ceramic side of the interface are exclusively anion or cation[28]. For example, the obtained interface relation can be designated as Ag (111)/SnO_2 (200), that the related electron diffraction pattern is shown in Fig. 3(b) and the corresponding crystal plane indexes are also indicated as well. Figure 3(a) shows the HRTEM image of the interface, and one can see that it is absence of any precipitated compounds across the interface. The gray contrast in Fig. 3(b) is mainly attributed to the interface strain, which is recorded to the atomic mismatch at the interface. The observed lattice contrast images are clear and very sharp across the interface which implies the absence of the precipitated phase. Near the interface, the experimentally determined lattice spacing of several different crystal planes both for Ag and SnO_2 are labeled in Fig. 3(c). For instance, the distance between (002) plane of SnO_2 matrix is 0.1566 nm, very close to the value calculated by using experimental lattice constant of bulk material. The implementation of inter-atomic potential models for non-polar interfaces[28] may be relatively easier because the interface interactions are smaller compared to those in the constituent bulk metal and bulk ceramic.

In this section, according to the results by HRTEM, the interface structure of silver and tin oxide is built at atomic scale and performed to relax firstly. The thickness of the analyzed nano-structure interface of Ag (111)/SnO_2 (200) is about 10 nm, which includes 16 layers of atoms, 6 layers of Ag and 10 layers of SnO_2 (the total number layers of Sn and O atoms). In fact, atom layers outside of 16 layers are fixed. The equilibrium atomic positions of the interface cell are obtained by the minimizing the total energy of the structure[19]. In different situation, much of the states are metastable, and the result of the lowest energy is selected to calculate the properties[18]. Figure 6(a) shows the initial model of the Ag (111)/SnO_2 (200) interface structure, and the corresponding thickness is about 10 nm. The atomic configurations of the studied model matches well with the HRTEM results as shown in Fig. 3. The oxygen terminated (200) surface is selected because the related experimental results clearly indicated that Sn terminated surface is unstable during the internal oxidation process. Only
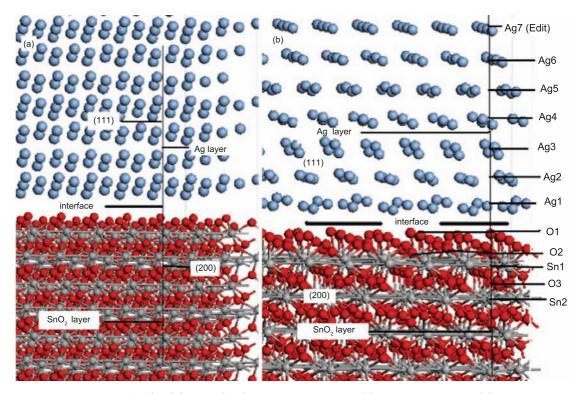
Fig. 6 The model of Ag (111)/ SnO$_2$ (200) interface structure: (a) before relaxation, (b) after relaxation

O terminated (200) interface in the Ag/SnO$_2$ composite is frequently observed. Large positional distortions are observed for the atoms across the interface by many previous investigations and this effect decays exponentially from the interface. The model here we used contains sufficient layers both for SnO$_2$ and Ag matrix in order to reduce the interactions between the image cells and the bulk in the same cell.

The obtained equilibrium atomic structure is illustrated in Fig. 6(b). The atomic positions at the interface are heavily distorted when compared with the initial state of Fig. 3(a). However, after relaxation, atoms near the interface matched badly and some empty bonds presented in SnO$_2$ layers. It is interesting that the formerly two fold coordinated O atoms on SnO$_2$ side at the interface were aligned vertically and intended to bond with Ag. By analyzing, the bond of O1 atom was fastigiated at first; nevertheless, in order to capture more electrons and go to the lowest energy for the stable structure it entirely trended to close up Ag atoms after relaxation. In addition, the hypo-near neighbors O$_2$ atoms had moved outside of the matrix to the interface, too. The same trend was also observed in Ag atoms near the interface. For instance, the distance between the Ag and O atom was 0.5328 nm at first, but it shifted to 0.4224 nm after relaxation. This trend was also affected to the other O atoms near the interface. On the other hand, compared to O atoms, the atomic positions of Sn atoms in the SnO$_2$ lattice were very insensitive to the relaxations and only small displacements are obtained. This phenomenon explained the matched badly inter-face and the bond of Sn-O turned longer and longer, such as the bond of Sn-O1 is 0.1801 to 0.1989 nm, the Sn-O2 is 0.1684 to 0.1884 nm, respectively.

Table 1 illustrates the calculated mean square atomic displacements of distinct atoms near the interface. We have concluded that the atomic positions of Ag are modified greatly during the optimization. This is consistent with the results which can be clearly seen from Fig. 6(b). The results of Ag layers near the interface after relaxation, show that the nearest layer of interface was reconstructed seriously and the periodic Ag lattice was broken completely. In Fig. 6(b), the nearest six Ag layers moved to the interface direction. The atoms were more near the interface, the displacements were bigger. Compared to the 6th layer and 7th layer (fixed), there is few change between the atomic positions of two layers. This result proved that the model of this paper was in agreement with the real condition of experiment. In a word, the relaxed structure was a type of transitional phases in metal/ceramic composite, in which the mismatch between the Ag and SnO$_2$ phases was declined. In Fig. 6(b), the symmetry of the Ag layers in the progress of relaxation were still kept well. Only atoms in horizontal direction were moved by a few displacements. However, the atoms in vertical direction were disorganized badly. When the atoms near the interface structure were confused seriously, the stress of the lattice improved quickly, and the properties of the composite might be changed enormously. The mean-square displacements of atoms could explain the movement of inside atoms in materials. From the

Table 1 Mean-square displacements of atoms on the interface in three-dimensional space

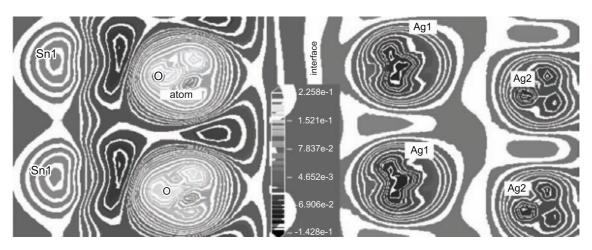|	Total u^2(in a.u)	xx u^2(in a.u)	yy u^2(in a.u)	zz u^2(in a.u)	xy u^2(in a.u)	xz u^2(in a.u)	yz u^2(in a.u)
Ag1	5.958289	0.690849	0.849027	4.118413	−0.3198	−0.82007	0.500262
Ag2	5.696986	1.74724	0.851665	3.098081	−0.13805	−0.35562	0.948951
Ag3	5.364194	0.989965	0.960529	3.4137	−0.04173	−0.02852	0.412339
Ag4	4.900222	1.193249	1.496462	2.210511	−0.03217	0.094036	−0.01717
Ag5	4.398377	0.722696	1.446716	2.228964	0.201786	−0.12775	−0.40038
O1	2.836353	0.008238	0.006275	2.521839	−0.0036	−0.11629	0.084119
O2	2.601914	0.002467	0.005791	2.593656	−0.00303	−0.07221	0.112144
O3	2.545328	0.003028	0.005332	2.536968	−0.00341	−0.0814	0.103356
Sn1	2.573747	0.00348	0.005171	2.565095	−0.00374	−0.08939	0.110748
Sn2	2.577378	0.002554	0.007008	2.567816	−0.00373	−0.07678	0.129824

Fig. 7 Electronic distribution of the Ag (111)/ SnO$_2$ (200) interface

above analysis, we can see the variational distance was Ag1>Ag2>Ag3>Ag4>Ag5 and this is in agreement with the conclusion of the front. By analyzing the position of O atom near the interface, the movements of empty O1 bonds were more than the bridge O$_2$ bonds, too.

The electric-conductivity of Ag/SnO$_2$ composite is determined by the interfacial states. The conduction shows more delocalized characteristics, which may affect the electron conductance at the interface. Figure 7 illustrates the calculated electron density distribution map of Ag/SnO$_2$ interface. The electron density is accumulated at different atoms and the density values are very small across the interface. In the interstitial regions of Ag far from the interface, the electron density values are larger than zero due to metallic bonds among Ag atoms. Sn-O bonds near the interface show ionic and covalent character. We can see that the electronic distribution of O atom is very thick and around the Sn and Ag atom is thinner. This is one of the characters of the metal/ceramic composite. In Fig. 7, we could see that the nearest Ag atom lost electron more than the hypo-near neighbor's atoms. All of the Ag atoms moved close to O atoms in the interface structure area. The electronic distributions were unsymmetrical, so the mechanical and conduc-

tive properties of the composite would be affected. Compared with Ag atom between interface and bulk, it was found that some of Ag atoms near the interface "captured" some electrons, which was considered the free electrons moved in the materials and the effect of interface, too. By analyzing the bonding near the interface, the O and Ag atom were not bonding. That was because the distance between Ag and O atom (>0.4 nm) was much longer than the longest bond length in the any of Ag$_x$O$_y$ compound. Because the structure near the interface was changed, the electronic wave function changed too, and the new electronic states would be presented in some interior of materials. Electron density changed acutely and a micro-electric field also formed in the whole material because of the interface structure. This may affect the electron motions and the related conductivity property of composite[28]. In conventional investigation, the interface was considered to resist the electronic transmission. But in this paper, we think not only the sizes and contents of reinforcements, but also the micro-electric field affected the conductivity property of composite. Generally, electron density distributes inequality, which leads to anisotropy in the cohesive interface. The results showed that the Ag/SnO$_2$ composite's interface was an ionic and cova-

lent bonding, which was stabilized and strong. However, the electronic distribution was inequality near the interface and the bonds were mostly of immovability, which led to less deformation ability of the material (ductile fracture was turned to brittle fracture). Because of the strong bonding in the interface, the tensile strength of the composite was high and the brittleness and toughness were improved, too. This explained why the mechanical property of the metal/ceramic materials was improved but the machining property declined by analyzing the electronic distribution between metal/ceramic interfaces.

5. Conclusions

The good mechanical and electrical performances of Ag/SnO_2 composite were achieved by reactive synthesis method in this paper. The micro structural feature was typical for the particle reinforced composites. The average particle size of SnO_2 in Ag/SnO_2 composite was near 50 nm and it was well dispersed in spherical shape. The HRTEM images revealed that the observed electric contact material of Ag/SnO_2 interface was absence of the precipitated phase and the lattice contrast across the interface was clear and sharp. The reactive Gibbs free energy per volume for each of probable reactions was evaluated. When the temperature increased up to 505 K, the process of synthesis of composites was replacement reaction between the solid particles. Nevertheless, in the temperature range of 505 K to 1200 K, these reactions were greatly enhanced by the existence of excessive O_2 atmosphere.

The electronic density distribution analysis of the interface showed the charges of Ag atoms transmit to O atoms and the conductivity of the material was also affected. The mean-square displacements of atoms near the interface showed that near the interface both Ag and SnO_2 layers were matched badly, besides this effect decayed rapidly far from the interface. No extra compounds expected such as Ag_xO_y formed at interface. Electron density changed acutely and a microelectric field also formed in the whole material due to the interface structure, and this might affect the electron motions and the related conductivity of composite. The electronic distribution was of inequality near the interface which explained why the mechanical property of the metal/ceramic materials was improved but the machining property declined.

REFERENCES

[1] P. Peng, C. Zheng, S. Han, Z. Jin and R. Yang: *J. Mater. Sci. Technol.,* 2003, **19**(1), 26.
[2] G. Profeta, A. Continenza and A. Freeman: *Phys. Rev. B,* 2001, **64**, 045303.
[3] G. Profeta, A. Blasetti, S. Picozzi, A. Continenza and A. Freeman: *Phys. Rev. B,* 2001, **64**, 235312.
[4] S.V. Dmitriev, T. Kitamura, J. Li, Y. Umeno, K. Yashiro and N. Yoshikawa: *Acta Mater.,* 2005, **53**, 1215.
[5] M. Raffi, F, Hussain, T, M. J. I. Akhter, A. Hameed and M. M. Hasan: *J. Mater. Sci. Technol.,* 2008, **24**(2), 192.
[6] K.M. Carling and E.A. Carter: *Acta Mater.,* 2007, **55**, 2791.
[7] S.V. Dmitriev, N. Yoshikawa, K. Masanori, T. Shingo and Y. Rui: *Acta Mater.,* 2004, **52**, 1959.
[8] E. Heifet, Y.F. Zhukovskii and E.A. Kotomin: *Chem. Phys. Lett.,* 1998, **283**, 395.
[9] J. Guo, L. Zhang, A. Xian and J.K. Shang: *J. Mater. Sci. Technol.,* 2007, **23**(6), 811.
[10] X.M. Liu, S.L. Wu, P.K Chub, C.Y. Chung, J. Zheng and S.L. Li: *Mater. Chem. Phys.,* 2006, **98**, 477.
[11] J.B. Wang, Y. Zhang, M.G. Yang, B.J. Ding and Z.M. Yang: *Mater. Sci. Eng. B,* 2006, **131**, 230.
[12] P.D. Padova, R. Larclprete, M. Mangiantini and M. Fanfoni: *J. Electron Spectrosc. Relat. Phenom.,* 1995, **76**, 499.
[13] J.C. Chen, J.L. Sun and X.L. Zhou: *Electron. Eng. Mater.,* 2002, **4**, 41.
[14] J. Feng, J.C. Chen and B. Xiao: *Rare Metal Mater. Eng.,* 2007, **36**, 174.
[15] K.H. Zhang, J.L. Sun, W.M, Guan and J.C. Chen: *Rare Metal Mater. Eng.,* 2006, **35**, 1581.
[16] M.W. Finnis, C. Kruse and U. Schiinberger: *Nanostructure Mater.,* 1995, **6**, 145.
[17] M.W. Finnis: *J. Phys.: Condensed Matter.,* 1996, **8**, 5811.
[18] J.M. Howe: *Mater. Sci. Eng. A,* 2006, **438-440**, 35.
[19] S. Mogck, B.J. Kooi and M.W. Finnis: *Phys. Rev. B,* 2004, **70**, 245427.
[20] S. Takeo, M. Katsuyuki, O. Hiromichi and H. Hideo: *Sci. Technol. Adv. Mater.,* 2003, **4**, 575.
[21] N.I. Medvedeva, Y.N. Gornostyrev, O.Y. Kontsevo and A.J. Freeman: *Acta Mater.,* 2004, **52**, 675.
[22] M.D. Segall, P.J.D. Lindan, M.J. Probert, C.J. Pickard, P.J. Hasnip, S.J. Clark and M.C. Payne: *J. Phys. Condens. Matter.,* 2002, **14**, 2717.
[23] P. Hohenberg and W. Kohn: *Phys. Rev. B,* 1964, **136**, 864.
[24] G. Kresse and D. Joubert: *Phys. Rev. B,* 1999, **59**, 1758.
[25] J.P. Perdew, K. Burke and M. Emzerhof: *Phys. Rev. Lett.,* 1996, **77**, 3865.
[26] Y.J. Liang, Y.C. Che and X.X. Liu: *Manual of Practical Inorganic Matter Thermodynamics*, Northeastern University Press, Shenyang, 1993. (in Chinese)
[27] C. Mallikaa, A.M. Edwin Suresh Rajb, K.S. Nagarajab and O.M. Sreedharan: *Thermochim. Acta,* 2001, **371**, 95.
[28] A. Chatterjee, S. Niwa and F. Mizukami: *J. Mol. Graph. Modell.,* 2005, **23**, 447.